

## THE INFLUENCE OF THE MICRO-ALLOYING ELEMENTS ON PHYSICAL AND STRUCTURAL CHARACTERISTICS OF THE SOME STEEL DESTINED FOR MANUFACTURING THE OIL PIPES

C. O. RUSĂNESCU<sup>1</sup>, M. RUSĂNESCU<sup>2</sup>, F. V. ANGHELINA<sup>3</sup>, V. BRATU<sup>3</sup>

<sup>1</sup>“Politehnica” University, Faculty of Biotechnical Systems Engineering Bucharest, Romania,

<sup>2</sup>Valplast Industrie Bucharest, Romania

<sup>3</sup>“Valahia” University of Târgoviște, Faculty of Materials Engineering and Mechanics,

18–24 Unirii Avenue, 130082, Târgoviște, România

E-mail: v\_bratu22@yahoo.com

*Received January 10, 2014*

*Abstract.* The present paper studies the influence of the microalloy on the characteristics of the some steel classes destined to manufacturing the oil pipes. Added to the realization of high report between the resistance characteristics and tenaciousness by using the fine granulation there can be obtained the rising of the capacity to weld of the steel, by reducing the content in carbon in order to realize the same level of resistance at breaking. Was used as a test for a hot torque reference steel (C-Mn) in the steel of investigation (C-Mn-V). We determined the characteristics of deformation and strain hardening coefficient for two strain rates at different temperatures torsion test.

*Keywords:* microalloyed steels, hardening coefficient, austenitic grain.

### 1. INTRODUCTION

The main purpose of microalloyed steels is to obtain a high tensile strength combined with good toughness. The mechanism by which the decrease in the change of properties is grain steel. Grain size greatly influence the tensile strength of the material. Grain size is influenced by a number of technological factors controlling indirectly controlling grain austenitic and ferritic. Thus, in addition to the element type of micro-alloyed steel, grain size is determined by the conditions of forming and heat treatment.

The main goal pursued by microalloyed vanadium in alloy steels is to influence their structure in a way that leads to improved mechanical characteristics.

The mechanisms that affect the metallurgical structure of the steel microalloyed with Vanadium are as follows [1]: binding interstitial elements (N, C) austenitic grain finish ferritic grain finishing results after austenite transformation;

delay dynamic and static recrystallization during hot processing, high temperature reflow process stop, slower rate of transformation of austenite, increasing stability comeback. Due to these mechanisms, vanadium micro-alloyed steels technologies used by processing parameters can control the growth resistance and toughness of products within certain limits.

Obtaining fine particles and uniformly dispersed in the solution by precipitation reaction, it is essential to use fine-grained steels. The literature indicates the maximum value of 50 Å precipitate diameter, size for which it acts as an inhibitor of grain [2].

This paper aims to achieve oil pipes with  $R_c > 540 \text{ N/mm}^2$ . In this group are included resistance levels J 55 (370–552 N/mm<sup>2</sup>) and N 80 (552–758 N/mm<sup>2</sup>). These two degrees now covers 70% of the oil pipe in the country.

In order to obtain the degree of strength characteristics of the normalized or standardized supplied from the heat of rolling, using C-Mn steel micro-alloyed with vanadium, vanadium is recommended to use it due to the action of hardening by precipitation [3, 4, 6].

## 2. MATERIALS AND METHODS

Based on knowledge of the chemical composition and metallographic structure of metallic materials can determine the physical, mechanical and technological properties.

Study of the structure of metals and alloys to metallographic microscope, are together with chemical analysis and determination of physico-mechanical properties, a basic research method of metallic materials. It allows highlighting the microscopic structure of these metallic materials, metallographic constituents (nature, shape, size, distribution, and so on) and the association of crystalline grains of the constituent phases.

Study of metallographic structure is important because it gives guidance on elaboration alloys, the heat treatment, the mechanical and thermo-chemical treatment, putting into evidence the invisible defects such as (microporosity, non-metallic inclusions, and so on).

The addition of a single element favourably influence only in a certain sense the properties of steels, while the complex alloying – preferred in current compositions of economical and high resistance steel – ensures a more efficient and concomitant influence on both the technological characteristics (deformation, weldability, hardenability, and so on) as well as the exploitation characteristics (increase in the mechanical strength, cold or hot, the fatigue strength, yield strength, toughness, and so on). This is explained by the fact that each alloying element is distributed differently between the phases existing in the steel structure.

In this regard, the paper studies the five samples taken from different types of steels of which OLT 65 is steel reference without microalloyed and J55 – fine grain steel with aluminum control and the other samples are alloyed with vanadium such as the: Grade D – steel microalloyed with vanadium, Grade E – vanadium microalloyed steel and aluminum control and 31VMn12 – microalloyed steel with vanadium.

Chemical composition of steel grades imposed for type OLT 65 considered as reference samples is specified in Table 1.

*Table 1*  
Chemical Composition (%)

Criteria	Min.	Max.
C	0.4000	0.5000
Mn	0.7000	1.0000
P	–	0.0400
S	–	0.0450
Si	0.1700	0.3500
Ni	–	0.3000
Cr	–	0.3000
Mo	–	0.0600
Cu	–	0.3000

*Carbon Equivalent:*

$$Ceq\ 1 = 0.69$$

$$PCM = 0.53$$

*Formulas:*

$$Ceq\ 1 = C + Mn/6 + Cr/5 + Mo/5 + V/5 + Cu/15 + Ni/15$$

$$PCM = C + Si/30 + (Mn + Cu + Cr)/20 + Ni/60 + Mo/15 + V/10 + 5 \cdot B.$$

Representative of the physical properties of steel grade OLT 65 to study, we mention (Table 2).

*Table 2*  
The representative physical properties of steel grade OLT 6

Density, $\rho$ [kg/dm <sup>3</sup> ]	Modulus of elasticity [GPa]	Poisson's coefficient, $\nu$
Value	Value	Value
7.72–8.00	190–210	0.27–0.30
7.80	202	0.27–0.30

Microstructures were visualized with a microscope of the type REICHERT assisted by a computer equipped with software for image analysis. The device is equipped with a high resolution digital camera Type Polaroid DMC 1E type TWAIN driver. Image analysis equipment, has a Frame Grabber type Matrix Meteor II.

Structural analyzes were carried out at 250 magnification to determine the appearance of the structure and grain size.

Cooling conditions for grain highlighting oxidation method (adopted in accordance with the carbon content of steel) were according to STAS 5490-80, samples were prepared according to STAS 4203.

Experimentation was conducted to determine temperature austenitising leading all studied steels austenitic grain size at the same warming to deformation.

Were retained for metallographic analysis reports only representative microstructures.

After cutting, the samples were submitted to grinding operations (primary grinding), and has been used for this purpose grinding machine MLG 11. The samples thereby processed were machined on the lathe to prevent embedding of abrasive particles in the test sample / tested.

For elemental analysis of the mentioned samples spectrometric technique was used, the tests were performed using the optical emission by electric spark spectrometer type Foundry-Master. This is an automatic facility designed elemental analysis of metallic materials and operates under a program (software) assist you in real time [12, 13, 14].



Fig. 1 – Optical emission by electric spark spectrometer type Foundry-Master.

**Characterization of the torsion test method.** Experimental comparative study of the behavior of materials under laboratory conditions was made using the hot torsion test facility SETARAM.

Torsion test stage has become one of the most used methods to determine the technological deformability of metallic materials.

The study hot deformability of the steel studied it is necessary to determine the influence of the chemical composition of the steel of the plasticity of the material, the determination of the influence accompanying the iron elements on the process of dynamic recrystallization and precipitation. Micro-alloyed elements influence the physical, mechanical and technological material characteristics as in the form of a solution in austenite as well as in the form of agglomerates. During the deformation, partial precipitated micro-alloyed elements influencing both the precipitated and dissolved in the solution, recrystallization of austenite. Heating the heat treatment in the austenitic steels behave differently depending on the micro-alloyed chemical element. Normalization of steel with chemical element vanadium or niobium, heating, growth of precipitates is approximately similar, but the cooling precipitation of vanadium is very high compared to that of niobium [8–11]. This demonstrates the specific property of hardening by precipitation of chemical element vanadium. Hardening by the precipitation over certain strength, toughness worsens with increased material strength characteristics. A micro-alloyed with chemical element niobium and vanadium is recommended for quenching and tempering, causing: austenite grain control of heating for hardening precipitates of Nb; hardening *via* precipitation of chemical element vanadium in annealing [4].

Torsion test allows to obtain experimental data based on the plastic behavior of the metal. This test allows the direct torque curve tangential-slip specific curve characterizing plastic behavior of the material. In practical measurements, material plasticity is assessed by studying its behavior in the specific strains greater than the elastic region where Hooke's law applies. In this specific deformation zone size depends not only on the initial and final pressure in the spring, but the way she went to reach the final value.

In terms of the characterization of the material, the plasticity is thought to maximum load that can be applied to a body without causing undue plastic deformation. Plasticity criterion to be expressed by such voltages to be applied to any tension.

During torsion test specimen is applied in a manner that is very close to the requests processes occurring in the actual deformation, the plastic flow is caused by the shear stress components.

### 3. RESULTS AND DISCUSSIONS

Five specimens machined steel grades were initially austenitising at 1150 °C and stirring maintained for 3 minutes, followed by cooling to a temperature programmed tests (800, 900, 1000 °C). They tried to torsion strength, steels used in practice for achieving resilience J 55: OLT 65 – Steel reference without microalloyed, J55 – fine grain steel with aluminum control, grade D – steel microalloyed with vanadium. And in the manufacture of degree N 80: Grade E –

vanadium microalloyed steel and aluminum control, and 31VMn12 – microalloyed steel with vanadium these steels are used in practice in order to achieve the degree of strength N 80.

The tests were carried out in air and at the time of breaking the test specimen was rapidly quenched part (1–3 s) to freeze the austenitic grain and the other cooled in still air.

The test in air followed achieve deformation in conditions as close to practice.

Deformation temperatures were established considering the conditions of the end of hot plastic deformation of pipes in various stages and technological flows and austenitic grain size determined in Fig. 4.

The torsion test results are shown in Table 4.

It was noticed the deformability steels according to the deformation temperature and influence how microalloyed deformation and cooling after deformation.

The chemical composition determinate by spectrometric investigation methods specified in the literature [12–20] for mentioned samples of steel is presented in Table 3.

Table 3

The chemical composition of the steels tried at torsion

Steel	Elements from composition, %													Degree of resistance
	C	Mn	Si	P	S	Cu	Cr	Ni	Mo	V	Al	N ppm	O ppm	
OLT 65	0,36	0,79	0,23	0,010	0,022	0,10	0,09	0,11	0,001	–	0,019	50	93	J 55
Grad D	0,40	0,66	0,28	0,010	0,017	0,20	0,008	0,05	0,001	0,12	0,016	60	69	
J 55	0,34	0,99	0,31	0,016	0,028	0,24	0,21	0,17	0,013	–	0,050	100	88	
Grad E	0,30	1,18	0,22	0,010	0,021	0,29	0,12	0,15	0,001	0,15	0,032	110	120	N 80
31VMn12	0,28	1,24	0,28	0,015	0,007	0,14	0,14	0,12	0,001	0,17	0,018	89	106	

Torsion test was executed on a machine SETARAM, at temperatures of 800, 900, 1000, 1100 °C with the strain rate of 0.05 and 3 s<sup>-1</sup>. During test were acquired in real time values moment torsion and the number of turns that were used to determine the equivalent values of stresses and strains. Mathematical processing was done in Windows system files final data were loaded into a spreadsheet program (Excel 7.0) and was defined area located between the beginning recrystallization ( $\varepsilon = 0$ ) and strain  $\varepsilon_m$  corresponding to the maximum equivalent stress. Given the following equivalent relations:

$$\sigma = K \cdot \varepsilon^n \quad (1)$$

$$\ln \sigma = \ln K + n \ln \varepsilon \quad (2)$$

$$Y = B + A X, \quad (3)$$

where  $n$  is the coefficient of hardening and is able to harden the material during the deformation,  $A$ ,  $B$  and  $K$  are constants were of the logarithm values  $\sigma$  and  $\varepsilon$ ,  $Y = \ln \sigma$ ,  $B = \ln K$ ,  $A = n$ ,  $X = \ln \varepsilon$ .

For each determination, the section between  $\varepsilon = 0$  and  $\varepsilon = \varepsilon_{\max}$ , the linear regression is applied so a single independent variable of the equation (3), thus obtaining the values of the constants  $A$  and  $B$  (given in Table 4), resulting in the final values of strain hardening coefficient  $n = A$ .

For this process to use the mathematical equations and other authors have presented their works mathematical algorithm [21]. Hardening coefficient values for the five steel grades studied in two strain rates (0.5 and 3 s<sup>-1</sup>) and three temperatures (800, 900, 1000 °C), allowed graphical representation aiming to highlight the quality of existing compositional influences.

As shown in Table 4, the statistical processing of the recorded data showed a good correlation of values  $\sigma = f(\varepsilon)$  (correlation coefficient  $r$  higher than 0.8). There were some exceptions due to shortcomings of the test. The values for  $\sigma$  and  $\varepsilon$ , in the deformation until the maximum voltage were calculated coefficient straight line:  $Y = B + A X$  obtained from the logarithms of the values that describes the curve variation of the form:  $\sigma = K \cdot \varepsilon^n$ .

In the equation, the coefficient of the variable  $X$  ( $A$ ) is the hardening coefficient  $n$  (Table 4). The values obtained for the coefficient of hardening, were drawn graphics for each material and test temperature and strain rate of 0.05 and 3 s<sup>-1</sup> in Fig. 2a and b.

The central heating temperature before testing was justified austenitic grain size in Fig. 4.

The results obtained are shown in Table 4.

Table 4

The obtained results at trial torsion

Steel	Temperature test [°C]	$\dot{\epsilon}$ [s <sup>-1</sup> ]	$\sigma_{\max}$ [daN/mm <sup>2</sup> ]	$\epsilon_{\max}$ [%]	$\epsilon_r$ [%]	Regression coefficient $r$	A	B
OLT 65	800	0.05	141.85	1.22	3.97	0.9628	0.243	4.887
	900		73.85	0.88	5.34	0.7755	0.098	4.267
	1000		56.28	1.05	10.05	0.3404	0.115	3.791
Grad D	800	0.05	141.43	1.14	9.50	0.8919	0.177	4.874
	900		91.77	0.92	9.26	0.9889	0.285	4.577
	1000		93.05	0.66	18.70	0.9130	0.210	4.512
J 55	800	0.05	177.24	0.51	2.70	0.9518	0.264	5.008
	900		103.23	0.82	4.84	0.9817	0.267	5.658
	1000		90.08	0.18	13.43	0.8955	0.177	4.747
Grad E	800	0.05	111.30	0.55	1.81	0.7816	0.497	5.198
	900		76.92	0.28	2.63	0.9347	0.543	5.116
	1000		122.33	0.84	5.46	0.9704	0.223	4.795
31 VMn12	800	0.05	177.08	0.76	2.19	0.9938	0.354	5.301
	900		122.12	0.85	3.83	0.9817	0.317	4.809
	1000		117.05	0.60	5.44	0.6730	0.127	4.788
OLT 65	800	3	204,83	0,84	13,97	0,8900	0,230	5,383
	900		166,01	0,66	23,48	0,6806	0,208	5,202
	1000		109,46	0,84	27,10	0,7150	0,264	4,798
Grad D	800	3	207,36	1,32	13,64	0,7358	0,233	5,346
	900		157,57	0,51	23,84	0,7529	0,158	5,158
	1000		106,92	0,81	36,14	0,7349	0,172	4,730
J 55	800	3	222,56	0,81	11,34	0,5827	0,096	5,391
	900		173,60	0,66	18,73	0,8339	0,142	5,203
	1000		116,21	0,66	23,66	0,6983	0,111	4,775
Grad E	800	3	180,34	1,18	10,04	0,7453	0,3	5,341
	900		173,60	0,99	11,16	0,8342	0,376	5,081
	1000		117,05	0,66	17,23	0,7121	0,170	4,849
31 VMn12	800	3	209,90	1,32	12,00	0,8576	0,171	5,315
	900		183,73	0,66	16,42	0,8709	0,237	5,290
	1000		123,80	0,51	33,69	0,4395	0,352	5,046



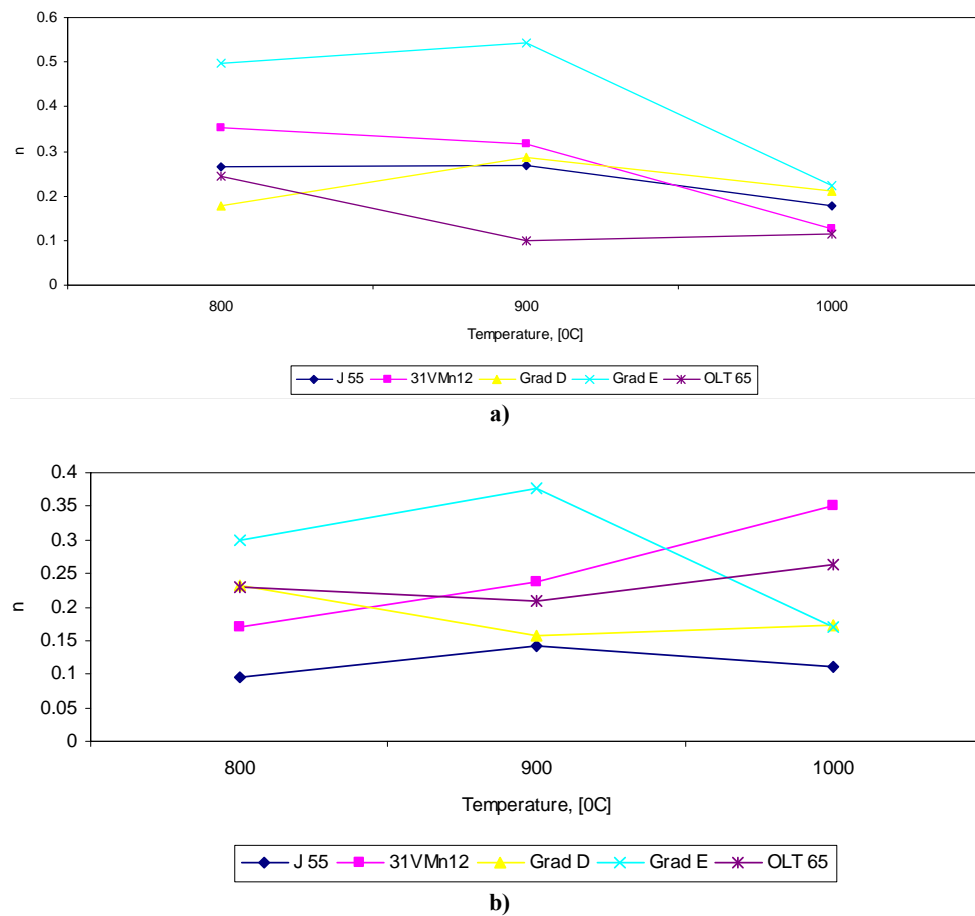


Fig. 2 – Hardening coefficient values  $n$  at different temperatures for each material tested at torsion: a)  $\dot{\epsilon} = 0.5 \text{ s}^{-1}$ ; b)  $\dot{\epsilon} = 3 \text{ s}^{-1}$ .

For the test to 1100 °C, the number of data acquired exceeded the capability of recording equipment. The test was carried out rupture, analyzing only the material structure. From the results recorded for all steels decreasing deformability between 100–800 °C test temperature decreases.

Hardening coefficient values, establish a relationship between voltage (resistance) and strain (plasticity) for the same test conditions.

Relatively large differences between the steels in the temperature range (900–1000 °C) is due to the different hot deformation behavior. Steel grade E, which has elements of vanadium micro-alloyed aluminum at 900 °C the highest capacity then declines rapidly hardening.

Hardening ability of steel to aluminum (J 55) does not change between 800–1000 °C, and the one with vanadium (31VMn12) shows an increase due to leaching of vanadium differential temperature rise test.

*Structural aspects of steels.* After the test up fracture, broken end of the sample cell water was cooled to analyze the austenite grain at the end of the deformation, and the fixed end has been allowed to cool in air.

The samples tested at 1100 °C steel J 55 grade E, 31VMn12 showed a completely recrystallized structure at the end of the water cooled, indicating a rapid crystallization by deformation at that temperature.

Austenitic grain size is 5–7 points (Fig. 3a).

The end of the cold air has a mixed structure of ferrite + perlite + bainite with a special feature.

In the deformed calibrated to the test in all cases we obtained a network structure ferrite steel cooling air J 55 (aluminum controlled 31 VMn 12 – and vanadium grade E – with vanadium and aluminum).

Uncalibrated broken and the sample cooled in air, then heated and cooled the undeformed but after the test under the same conditions, the microalloyed where the vanadium and the V+Al the ferrite pearlite structure with fine grains of ferrite.

Even in steel with aluminum (J 55) defines a protected network austenitic grain finer than that of deformity (Fig. 3d and 3e).

Explanation of these anomalies' may be based on data from the literature [22–27], namely.

a) the deformation zone (Fig. 3 b, d, f):

– high degree of deformation applied to the calibrated (up to rupture) increased the  $A_{r3}$ , transformation temperature on cooling, compared to this point in the uncalibrated;

– after deformation, in the calibrated recrystallization occurred suddenly, the austenite grain having time to grow up to  $A_{r3}$ , the precipitated particles are not prevented (solubilized in heating for deformation);

– when the temperature reached the  $A_{r3}$  began the limit  $\gamma \rightarrow \alpha$  transformation of austenite and ferrite grain was ordered networking between  $A_{r3}-A_{r1}$ ;

– high level of deformation of the low temperature precipitation of vanadium nitride VN, and AlN, precipitate probably occurring at the end of processing and after.

b) in the uncalibrated, undeformed:

– vanadium nitrides was completely dissolved and a part of the aluminum nitride;

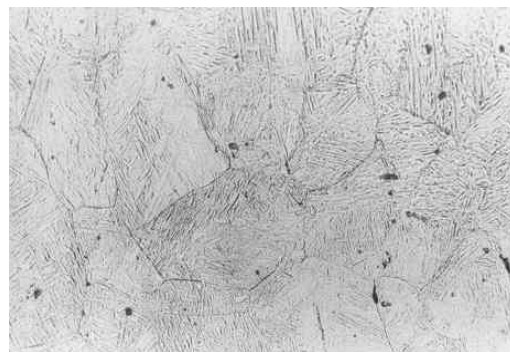
– the cooling air, vanadium steel VN precipitation occurred before the  $\gamma \rightarrow \alpha$  transformation temperature  $Ar_3$  not cause deformation.

As a result, beginning  $\gamma \rightarrow \alpha$  transformation occurred with germination of VN ferrite fine particles, resulting in the final fine ferrite grain structure.

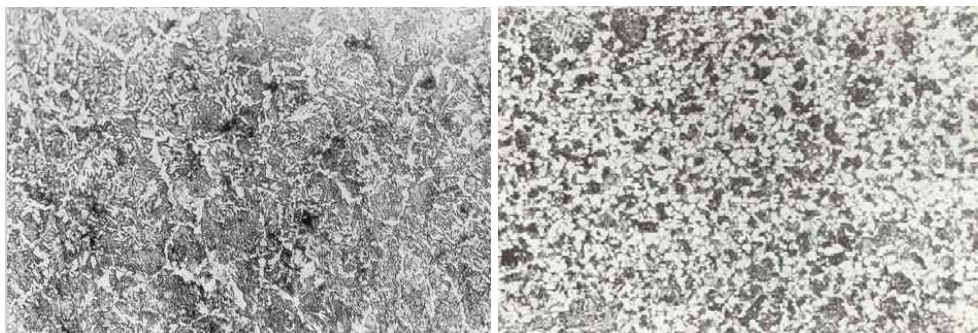
The steel with vanadium, but with aluminum, heating the presence of the AlN completely dissolved at 1150 °C to inhibit the growth of the austenitic grain to heating and / or cooling to  $Ar_3$ , but the precipitation of AlN for the cooling rate that was not sufficient to avoid the formation of the network ferrite, by separating them on the austenite grain.

The structural analysis at this stage confirmed the inhibitory role of grain for vanadium normalized recommended due to its specific mechanism of precipitation hardening.

Some authors have studied their works TEM images of carbon deposits and Surface Morphology of the samples was studied by Scanning Electron Microscope (SEM) [5, 7], others have studied by optical microscopy on the structural aspects of vanadium microalloyed steel but also other steel [5, 21, 28, 29, 30, 31, 32].



× 250  
a)



× 250  
b)

× 250  
c)

steel E

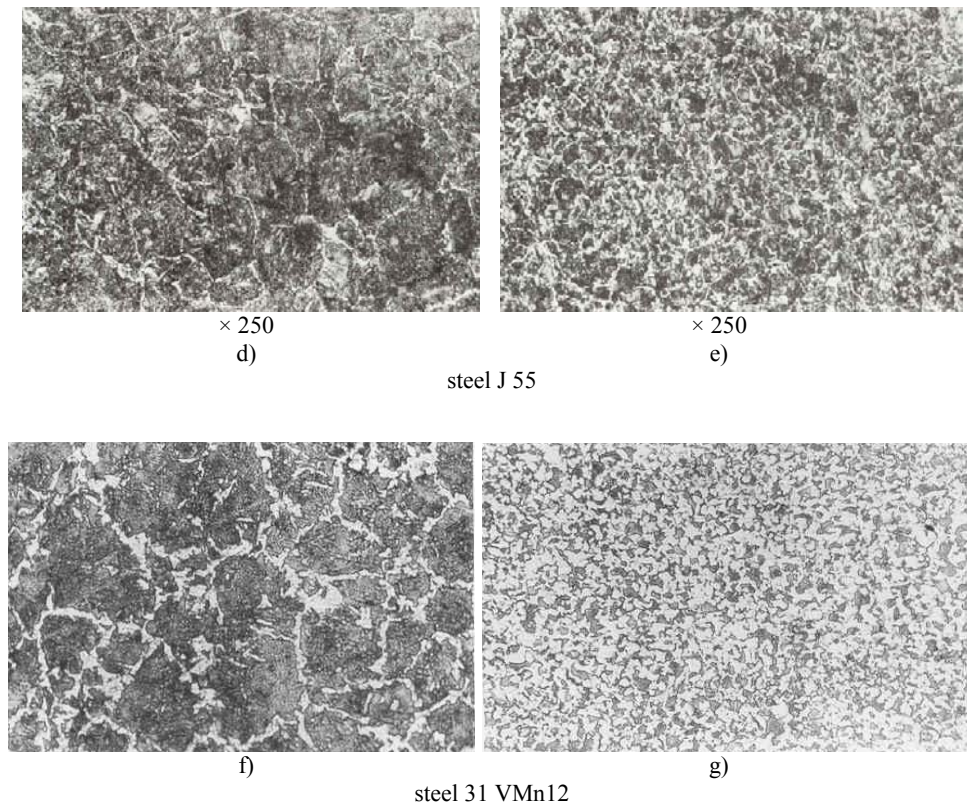
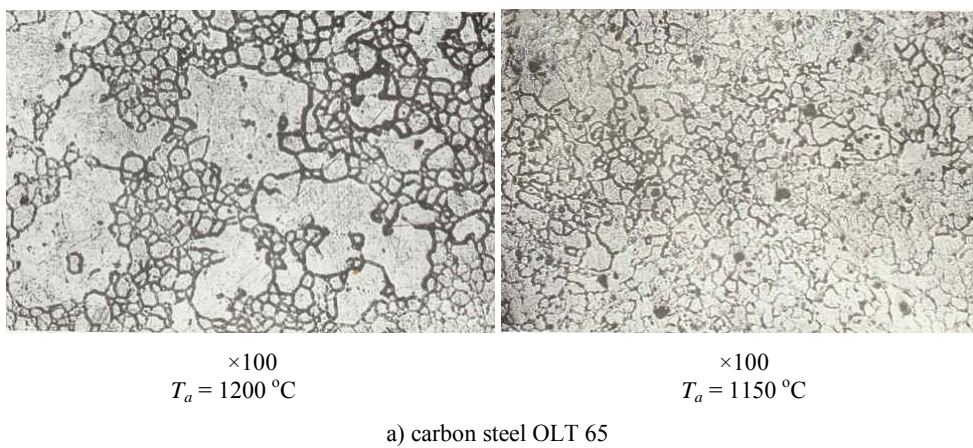
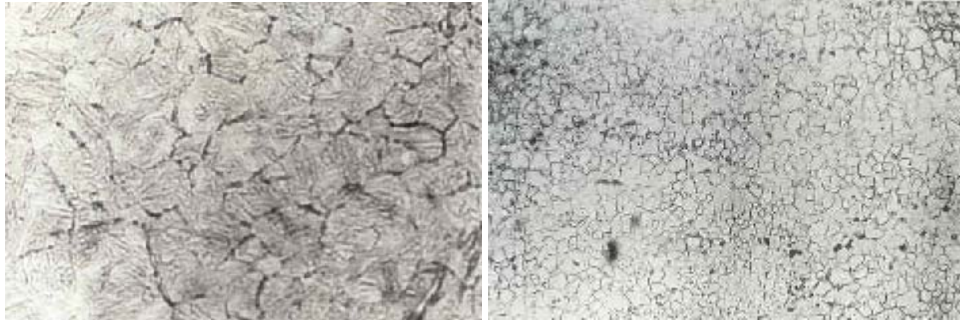


Fig. 3 – Structural aspects of vanadium microalloyed steel with aluminum compared to steel, to torsion at 1100 °C: a) – austenitic grain; b), d), f) – deformed end up breaking; c), e), g) – end uncalibrated, undeformed [6].





× 100  
 $T_a = 1200\text{ }^\circ\text{C}$

× 100  
 $T_a = 1150\text{ }^\circ\text{C}$

b) carbon steel, aluminum control J 55



× 100  
 $T_a = 1200\text{ }^\circ\text{C}$

× 100  
 $T_a = 1150\text{ }^\circ\text{C}$

c) steel microalloyed with vanadium

Fig. 4 (a-c) – Austenitic grain appearance when heated to different temperatures.

#### 4. CONCLUSIONS

It is also noted that the austenite grain increases with increasing heating temperature. The aim was to determine the manner in which the initial grain size of austenite (at the start of deformation) on the characteristics of deformability.

Before deformation, specimens of the examined steels were heated to a temperature of: 1200 and 1150 °C to see if there are differences in particle size of the heating temperature before deformation. As shown in the micrographs in Figure 4 at a temperature of 1200 °C austenitic grain size is not uniform.

On heating to 1150 °C was determined that the resulting austenitic grain size of vanadium microalloyed steel has a grain austenitic deformation beginning approximately two times lower than the reference steel OLT 65.

The samples tested at 1150 °C of steel 31VMn12 showed a completely recrystallized structure at the end of the water cooled, indicating a rapid crystallization at that temperature.

Austenitic grain size is 5–7 points (Fig. 4).

The end of the cold air has a mixed structure of ferrite + pearlite + bainite with a special feature.

Hardening coefficient values, establish a relationship between voltage and strain for the same test conditions. Relatively large differences between the steels in the temperature range (900–1000 °C) is due to the different hot deformation behavior.

Steel grade E, which has elements of vanadium micro-alloyed aluminum at 900 °C the highest capacity of hardening which then decreases sharply.

Hardening ability of steel to aluminum (J 55) not change between 800–1000 °C, and the one with vanadium (31VMn12) shows an increase due to differential solubility of vanadium in the high temperature test.

Choosing the type of micro-alloyed steel and should consider obtaining material toughness.

To ensure the toughness is necessary to reduce the carbon content of the steel, offset by an increase in manganese content. It can be experience the value of carbon equivalent  $C_{ech}$  max carbon 0.2 % and manganese max. 15 %.

Toughness control shall be implemented by micro-alloyed fine grain with V, Nb or Ti.

If the characteristics of the pipe socket is to achieve high J55, directly from the rolling heat, it is recommended to experience two solutions:

- microalloyed with vanadium V = 0.1–0.2 % and aluminum control;
- microalloyed with niobium and aluminum control (Nb < 0.05 %; Al = 0.02 – 0.05 %).

For the control of toughness and reduced anisotropy of the steel it is necessary to use low sulfur and phosphorus.

#### REFERENCES

1. O. Cuida, *Influence of trace elements and micro-alloyed steels on plasticity*, Image Publishing, 2000.
2. J. Humbert, B. Bergman, *Le concept de taux de déformation efficace additif en laminage contrôlé*, Revue de Metallurgie, CIT, 1981.
3. J.D. Michel, *Etude de la précipitation dynamique de Nb (CN) VN et AlN dans l'austenite d'aciers à bas carbone*, Revue de Metallurgie, oct. 1981.
4. J.D. Medina, *Static Recrystallization in Austenite and its Influence on Microstructural Changes in C-Mn Steel and Vanadium Microalloyed Steel at the Hot Strip Mill*, ISIJ, 1993.
5. C.O. Rusănescu, D. Stoica, *Mathematical model for calculating carbon dioxide catalyst and without catalyst engine*, Metalurgia International, 3, 81–83 (2013).
6. C.O. Burcea, PhD Thesis, Bucharest, 2003.

7. V.M. Sivakumar, A.Z. Abdullah, A.R. Mohamed, S.P. Chai, *Studies on carbon nanotube synthesis via methane cvd process using COOX as catalyst on carbon supports*, Digest Journal of Nanomaterials and Biostructures **5**, 3, 691–698 (2010).
8. T.M. Hoogendoorn & M.J. Spanraft, *Quantifying the Effect of Microalloy Elements on Structures during Processing*, Microalloying, 1975, P75-89.
9. F.S. Crawford Jr., Waves; Barkeley, *Physics Course*, Volume 3, 1968.
10. R.C. Brundle, C.A. Evans Jr., S. Wilson (Eds.), *Encyclopedia of Materials Characterization – Surfaces, Interfaces, Thin Films*, Butterworth-Heinemann, 1992.
11. D. Apostol, V. Damian, P. Logofatu, *Romanian Reports in Physics* **60**, 3, pp. 815–828 (2008).
12. K.A.Slickers, *Spectrochemical analysis in the metallurgical industry*, Pure&App/Chem. **65**, 12, pp. 2443–2452 (1993).
13. P. Walters, *Historical Advances in Spark Emission Spectroscopy*, Applied Spectroscopy, **23**, 4 (1969).
14. F.V. Anghelina, Ion V. Popescu, V. Bratu, E. Stoian, *SEM-EDAX and optical microscopy investigations of sparked-in spots on AES analyzed steel*, Proceeding AEE'10, Proceedings of the 9th WSEAS International Conference on Applications of Electrical Engineering, World Scientific and Engineering Academy and Society (WSEAS), Malaysia, Penang, 23–25 March 2010.
15. C.L. Sava, N. Rezlescu, *Determination of soluble and insoluble compounds in metals with spectrolab*, Romanian Reports in Physics **58**, 2, pp. 159–171 (2006).
16. K. A. Slickers, *Determination of soluble and insoluble compounds in metals with Spectrolab*, Application Report **35**, Germany, 1992.
17. Ion V. Popescu, I. Pencea, V.F. Anghelina, M. Branzei, F. Miculescu, C. Macris, C. Petre, *New Proves Concerning Streamer Mechanism of Vaporization and Sputtering of a Stainless Steel During Sparking for Optical Emmision Spectroscopical Analysis*, Romanian Reports in Physics, **63**, 3, 823–838 (2011).
18. I. Pencea, C.E. Sfat, F.V. Anghelina, *Uncertainty estimation for SDAR-OES internal standard method*, Scientific Bulletin of UPB Bucuresti, Series A – Applied Mathematics and Physics **72**, 1, 103–112 (2010).
19. A.F. Danet, *Analiza instrumentala – Partea I*, Univ. of Bucharest, Press 2010.
20. C.R. Blanchard, *Atomic force microscopy – The chemical educator*, Springer-Verlag, New York Inc., 1996.
21. C.O. Rusănescu, M. Rusănescu, F.V. Anghelina, *Study of the hot deformability of microalloyed steels using torsion tests*, Journal of optoelectronics and advanced materials **15**, 7–8, 724–729 1454–4164.
22. J.L. Bobet, S. Pechev, B. Chevalier and B. Darriet, *J. Alloys Compounds* **267**, 136 (1998).
23. M. Pugaczowa-Michalska, A. Kowalczyk, G. Chelkowska and T. Tolinski, *J. Alloys Compounds* **385**, 44 (2004).
24. P. Vlaic, N. Bucur, C. Lazar and E. Burzo, *J. Opt. Adv. Mat.* **8**, 490 (2006).
25. K. Kapoor, K. Muralidharan, N. Saratchanran, *Microstructure evolution and tensile properties of Zr-2.5%Nb pressure tube processed from billets with different microstructures*, Journal of Material Engineering and Performance **1**, 8, 61 (1999).
26. Grigore, M., Koncsag C., Ioan (Culea), C., *The characterisation, disposal and neutralization of the sludge proceeding from an oil refinery*, Chemical Industry and Environment V Conference, Vienna, 3–5 May 2006.
27. R.N. Singh, K. Kishore, A.K. Singh, and T.K. Sinha, *Microstructural Instability and superplasticity in a Zr-2.5%wtNb pressure tube alloy*, Metallurgical and Material Transactions A, Physical Metallurgy and Materials Science **32**, 11, 2827 (2001).

28. C.O. Rusănescu and M. Rusănescu, *The stress-strain curves determined for microalloy steel with V determined on the torsion tests*, *Metalurgia* **59**, 1, 38–44 (2007).
29. F.V. Anghelina, D.N. Ungureanu, V. Bratu, I.N. Popescu, C.O. Rusănescu, *Fine structure analysis of biocompatible ceramic materials based hydroxyapatite and metallic biomaterials 316L*, *Applied Surface Science* <http://dx.doi.org/10.1016/j.apsusc.2013.06.102>, [www.elsevier.com/locate/apsusc](http://www.elsevier.com/locate/apsusc).
30. S.F. Medina, P. Fabregue-J. *Mater. Sci.* **26** (1991).
31. L. Dinescu, C. Miron, E. Barna, *Rom. Rep. in Physics* **63**, 2, 557–566 (2011).
32. C.G. Bostan, N. Dina, M. Bulgariu, S. Craciun, M. Dafinei, C. Chitu, I. Staicu, S. Antohe, *Romanian Reports in Physics* **63**, 2, 543–556 (2011).